Hα MANIFESTATION OF AN ENERGETIC LIMB FLARE, JUNE 21, 1980

MARIE K. McCABE

Institute for Astronomy, University of Hawaii

(Received 29 October, 1984; in revised form 19 April, 1985)

Abstract. The Hα observations of a limb flare, which were associated with exceptional gamma-ray and hard X-ray emission, are presented and discussed. The good spatial and temporal resolution of the Hα data allow us to investigate the detailed structure of the elevated flare loops and the intensity variations of the loops, footpoints and surrounding chromosphere during each phase of the flare event. A delay time of ≈ 12 s was found between at least one of the hard X-ray (28–485 keV) peaks and corresponding Hα intensity maximum at a loop footpoint. A comparison is made between this event and another well-observed limb flare with many similar characteristics to seek evidence for the large difference in their levels of energy release.

1. Introduction

One of the most outstanding events observed during the Solar Maximum Mission (SMM) occurred at the west limb of the Sun on June 21, 1980. Following the impulsive photon emission which lasted for about one minute, energetic solar neutrons (>50 MeV) were detected at the Earth by the Gamma Ray Experiment (GRE) on the SMM satellite (Chupp *et al.*, 1982). Observations were also made with the SMM Hard X-ray Burst Spectrometer (HXRBS) – see Orwig *et al.* (1981) for instrument details – but the imaging instruments on the satellite were pointed to a different region on the Sun. Consequently, the only well-resolved spatial information available during the short impulsive phase came from ground-based Hα filtergrams. Microwave bursts were reported by Nakajima *et al.* (1983) and radio observations of type III, II, and IV bursts were observed at Culgoora (Robinson *et al.*, 1983). Intense white-light emission was seen above the limb (Harvey and Duvall, 1983) in association with the flare, and a coronal transient was observed with the SMM coronagraph polarimeter some hours later. In this paper we discuss the Hα manifestation of the flare which we attribute to a small compact system of loops above the limb and which displayed bright footpoints during the impulsive phase (1 min) followed by the development of less intense loops during the next 10 min and a mass ejection into the low corona.

It is well recognized that the Hα emission associated with the impulsive phase of X-ray flares originates in bright kernels situated on either side of the magnetic inversion line in regions of opposite polarity (Kane *et al.*, 1980, and references therein), and is characterized by broad Hα line profiles. On the solar disk, the positions of the flare kernels are best observed on Hα off-band exposures; the relationship to magnetic field structure is obtained from comparison with photospheric magnetograms (Vorpahl, 1972). For flares at the limb, while the magnetic field configuration is not observable, the vertical extension and loop structure of the flare are visible and provide information regarding the height of the radiation excited by flare electrons.

Solar Physics **98** (1985) 127–140. 0038–0938/85.15

Studies of the relative timing of solar flare emissions by comparing Hα and X-ray light curves have not been entirely consistent. Vorpahl (1972) found a time delay of 20–25 s between X-ray and corresponding optical peaks, while Zirin (1978) concluded that Hα emission and hard X-ray bursts were virtually simultaneous. For June 21, we have examined the Hα light curves at different intensity levels and compared them with both the integrated high (28–485 keV) and the lower (28–55 keV) energy channels of HXRBS and show a delay of ≈ 12 s for the brightest parts of the Hα kernels.

The observations and their analysis are presented in Section 2 and Section 3; the development of the event is summarized in Section 4 along with a discussion of characteristics which may be associated with flares that have high energy components.

2. Observations

On June 21, 1980, the Hα high-resolution telescope at Mees Solar Observatory, like the SMM instruments with pointing controls, was directed toward disk center, where an active center produced a large two-ribbon flare at 00 : 30 UT. Before the long-lived event had faded, a small bright flare appeared at the northwest limb and was recorded on the Hα full disk patrol instrument. Thus, the observations of the compact, highly energetic limb event were limited to these satellite and ground-based experiments which had full disk coverage and consequently relatively low or no spatial resolution. Hα (bandpass 0.5 Å) exposures were recorded continuously from June 20, 17 : 25 UT to June 21, 03 : 02 UT, with the rate of 2 frames/min increased to 5/min at 01 : 15 UT and to 10/min at 01 : 26 UT. The Hα flare commenced at 01 : 16 UT as an elevated bright point in a mound that had developed during the previous few minutes at N18 in Hale region 16898. The time-history of the flare is shown in Figure 1, which includes each exposure during the impulsive phase (01 : 18 : 31–01 : 19 : 55 UT) and selected frames from the rise and decay periods. The flare consisted of low-lying loops – two of which can be seen resolved at 01 : 17 : 31 UT – during the early stages. The intensity increased rapidly with strong emission near the footpoints in the chromosphere for ≈ 1 min. Progressively, other loops appeared, but were less intense and more inclined from the radial direction (e.g., 01 : 24 : 26, 01 : 26 : 22 UT).

At 01 : 25 UT the 10-cm coronagraph which incorporates a broadband Hα filter (FWHM 7.5 Å) was switched on to record the flare-associated prominence activity. Sequences of exposures (0.5, 1.0, 3.0 s) were taken at 0.5 min intervals until 02 : 39 UT, with a break between 01 : 34 and 01 : 56 UT. In addition, a few exposures were made with the green line 10-cm coronagraph using a narrowband interference filter (FWHM 1.5 Å) centered on Fe XIV ($\lambda 5303$) which detects coronal emission at $T \approx 1\text{–}2 \times 10^6$ K. The Hα coronagraph pictures in Figure 2 display the post-flare expansion of material into the corona. The first frame taken some hours before the flare shows the continual coronal activity typically seen above active regions, while the $\lambda 5303$ exposure at the same time displayed a coronal enhancement with diffuse loop structures.

Although the Hα emission during the flare event came from a relatively small area (see Figure 1), careful examination of the original film indicated that it included bright centers

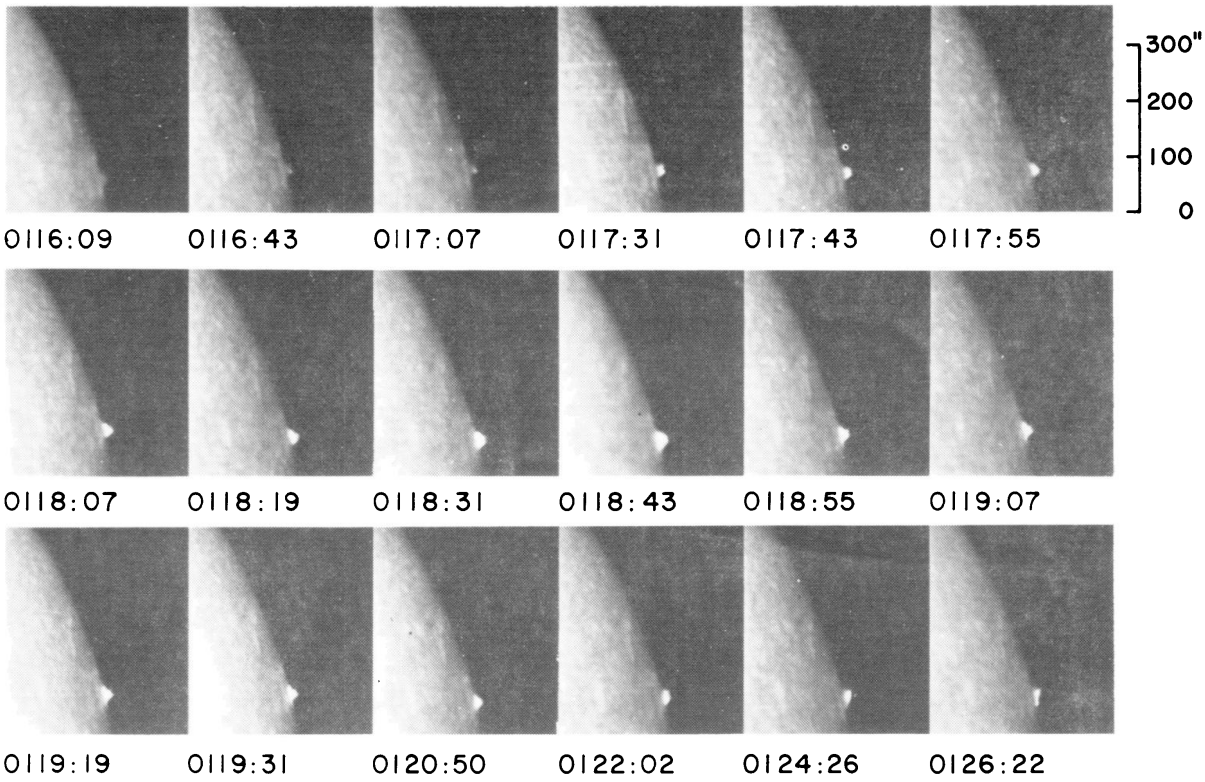

Fig. 1. Hα (0.5 Å) filtergrams of June 21, 1980 limb flare. The X-ray impulsive phase was during the period between 01 : 18 : 15 and 01 : 19 : 15 UT.

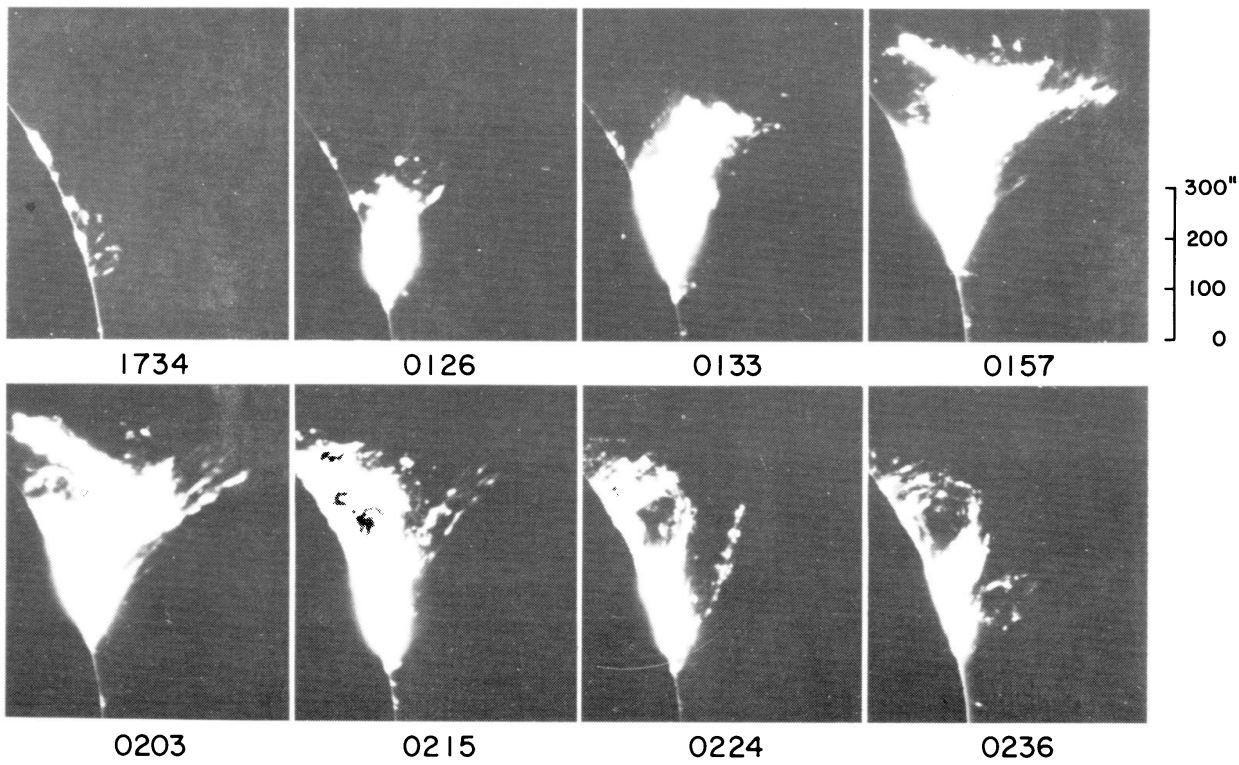

Fig. 2. Hα (7.5 Å) coronagraph filtergrams of mass ejection, June 20–21, 1980. The first frame shows limb activity eight hours prior to the flare event.

which changed in intensity, particularly during the impulsive phase, along with variations in the associated loop structures. Microdensitometer raster scans were made of the flare region for each exposure from 01 : 16 to 01 : 20 UT and on selected frames during the decay phase. Similar scans were made of a sunspot region – at a fixed distance – to correct for position errors and at Sun center to correct for variations of sky transparency during the observing period. The results are shown in Figure 3, where intensity contours are plotted; the intensity (I/I_0) is expressed in terms of the average Hα intensity of the quiet region at the center of the Sun on each frame. The square scanning aperture measured 12 μm on a side, and the step size was 12 μm (1.6 arc sec on the Sun), so that each contour map represents a region 42 × 64 arc sec^2. Due to the exposure characteristics, it was difficult to define an exact position of the solar limb on the contour maps. The film contrast is relatively low for the chromosphere near the limb, because the exposure time was selected so that flares might be recorded with high contrast but without saturating the film. A series of scans were made across the limb away from the active region and the inflection point of the intensity curve corresponded to a level of 0.4 I_0; the position of this contour is shown by the dashed line in Figure 3. Four of the raster scans were repeated to test the repeatability of film registration on the micro-

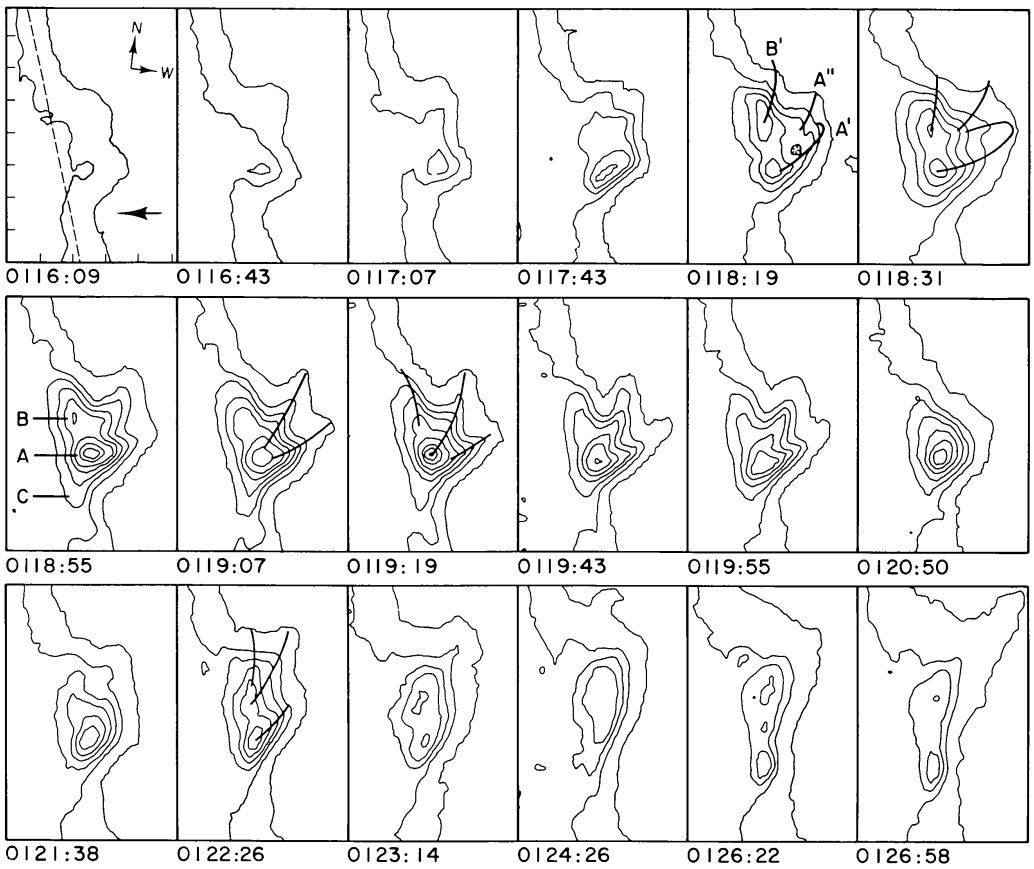

Fig. 3. Contour plots of limb flare. The levels correspond to 0.25, 0.50, 0.75, 1.00, 1.25, 2.00, 2.50, 3.00 of the average Hα intensity at Sun center for each scanning pixel (1.6 arc sec). Frame size is 42″ and tick-marks are at 8 arc sec intervals. The sunspot location is indicated by the arrow on the first frame.

densitometer and the photometric accuracy. The positions of maximum intensity changed by no more than 1.6 arc sec and the mean variation of intensity at these positions was 1.7 ($\pm$ 1.4)%.

3. Analysis

3.1. The active region and flare location

Observations of flares at or near the solar limb are important for studying the structure of component loops and the source of flare emission above the limb, but projection effects make for uncertainty in the position of the flare with respect to the existing plage, sunspot and magnetic field configurations. However, for the June 21 event, due to the stability of the active region during the latter half of its disk passage, it is possible to make a reasonable estimate of the flare location and of the probability that the footpoints were situated on the visible hemisphere.

Region 16898 produced many small flares as it moved across the disk until June 15; subsequently only five faint subflares were reported until the energetic event (*Solar Geophysical Data*, 1982). At central meridian passage (June 14) the region included two bipolar sunspot groups directly north and south of each other; by June 18 the southern group had decayed and the major spot was in the forward part of the leading positive magnetic field. Hα filtergrams on June 18 (Figure 4) and following days show that active region features lay mostly to the east of this sunspot while the chromosphere was typically quiet over an area extending 30° further west. Calculations indicate that the sunspot would have been at W88 at the time of the flare, and observations some hours beforehand (Figure 4) confirm this fact since the spot could be detected at the limb on the filtergrams taken at that time. As the flare loops developed just north of the sunspot in the plane of the sky, it can be concluded that the emission would be expected to originate on the visible disk even though there could be additional footpoints behind the limb.

3.2. The pre-impulsive phase 01 : 16 : 21–01 : 18 : 31 UT

During several hours prior to the flare there were sporadic shortlived brightenings in the active region at the limb and changes in the Hα and coronal features above it. By about 01 : 10 UT an elevated cloud had formed adjacent and to the north of the sunspot. It had a double structure, and a small bright kernel $\approx$5 arc sec in diameter developed 10 arc sec above the limb in the lower branch; the kernel became elongated in the form of an edge-on – i.e., the plane of the loop perpendicular to the plane of the sky – loop A' (Figure 3) but with no emission seen against the disk (01 : 17 : 43 UT). A similar but less intense loop B' in the upper branch was evident at 01 : 17 : 31 UT and showed a curvature to the north, while a third center became enhanced between these two features and higher up by 01 : 17 : 43 (loop A''). The three identified loops are sketched on the contour plot at 01 : 18 : 19 UT in Figure 3. At that time there was a change in A' with the emission concentrated near the limb while a depletion appeared above it, suggesting that the loop had become reorientated or reconnected, presenting a more face-on aspect.

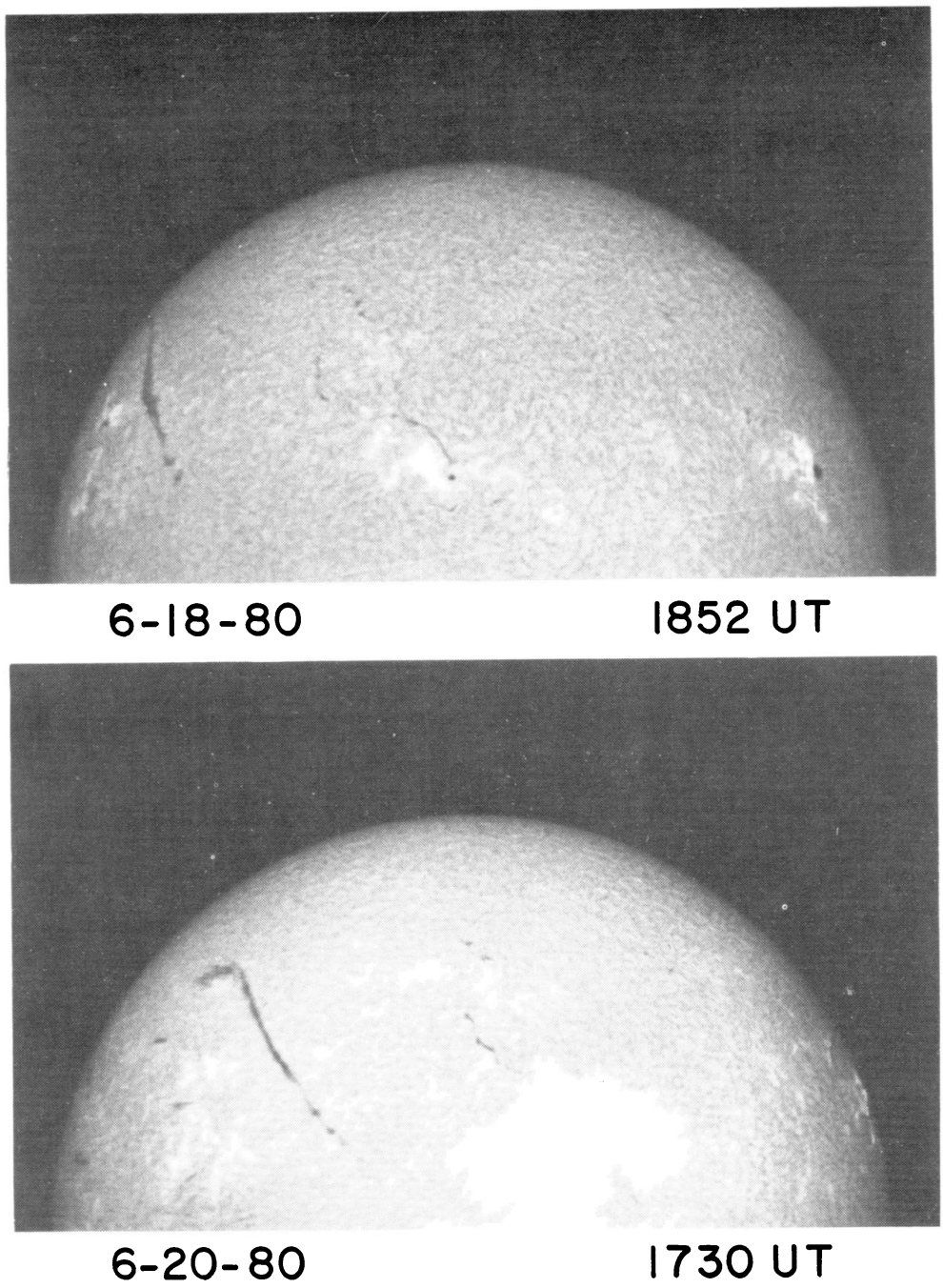

Fig. 4. Hα (0.5 Å) filtergrams of the active region on June 18 at ≈60° W and on June 20 near the solar limb, when the sunspot is still visible against the disk. Solar north is at the top and west to the right of each frame.

This loop can be seen to have extended in height in the next frame at 01 : 18 : 31 UT after which the top was no longer visible.

3.3. The impulsive phase 01 : 18 : 31–01 : 19 : 55 UT

The contour plots show that the Hα intensity increases during the flare impulsive phase were associated with the area *A* (Figure 3), while there was a more gradual rise and fall at *B*. The map at 01 : 18 : 43 UT has been excluded because the image was blurred due

to bad seeing (see Figure 1). At the first major intensity peak (01 : 18 : 55 UT) the two loops A' and A'' were distinguished, with strong emission from the footpoint of A', which remained confined. The loop A'', however, had extended and brightened. In the following frame the emission at area A has decreased, but the shape of the innermost contour suggests that loop A'' has brightened near its footpoint. At 01 : 19 : 19 UT the second emission peak occurred at A. Careful examination of the original film confirmed that the two bright centers were not quite co-spatial and indicated that both loops (A', A'') contributed to the impulsive event. During this period, there was extensive brightening in the chromosphere spreading on to the disk below the flare loops and first seen at 01 : 18 : 31 UT; an area at C showed a short increase in brightness and a small spike indicative of the appearance of another loop structure. It is possible that the bright footpoint of this loop contributed to a minor peak detected in X-rays between the major ones (Figure 4a). From 01 : 19 : 19 through 01 : 19 : 55 UT the loops A' and A'' became more defined as they brightened from the footpoints extending out into the corona; the top of A'' seemed to break off as though material were ejected.

3.4. The decay phase

The intensity of the loop footpoint at A had decreased to 50% maximum at 01 : 20 UT, and by 01 : 21 UT the extended emission region on the disk disappeared. The emission above the limb was more diffuse with little evidence of the previous loop formations. Subsequently at least three new loops developed and decayed at and north of the original A'; they were more inclined towards the limb away from the sunspot (see Figure 1; 01 : 22 : 02, 01 : 24 : 26 and Figure 3; 01 : 22 : 26 UT). At 01 : 26 : 58 UT one of them had extended info the corona to a greater height than the earlier loops. An interesting structure was the later brightening of a small but distinct low-lying structure at 01 : 26 : 22 UT (see Figure 1); like the footpoints of A' and A'' it was close to the sunspot. Its appearance correlated in time with a secondary X-ray burst. The region returned to the pre-flare level of activity at about 01 : 30 UT with continuing occasional small brightening at the limb.

3.5. Coronal effects

The flare was followed by Hα mass ejection into the corona. The average radial velocity of expansion was 300 km s^{-1} for the bulk of the material reaching 280 000 km above the limb; a few fragments escaped with velocities up to 500 km s^{-1} and were detected to a maximum height of 330 000 km. It is possible that more fragments were ejected before coronagraph observations commenced at 01 : 26 UT, but, assuming a high initial velocity of 1000 km s^{-1} at the time of flare maximum, they would have attained a height of 420 000 km and so remained in the field of view; there was no such evidence even on the longest exposures. After the data gap (01 : 34–01 : 56 UT) all the visible material was seen to fall back to the solar surface, either along the path of ejection or in the form of arches along the limb to a distance of 30° in position angle from the flare site. These structures appear as radial striations in the north projection from the material above the flare site and suggest an arcade of loops along the neutral line.

A coronal transient associated with the event was listed by Sawyer (1982) among events observed with the SMM Coronagraph/Polarimeter experiment. Three images obtained between 04 : 10 and 04 : 15 UT showed a transient in the north quadrant near the NW boundary of the field. Parts of the transient south of N50 were not observed until 20 min later, when a series of W quadrant images suggests that a cloud of material had been thrown out. The velocity estimated from measurements at a sharp edge at the top of the transient and probably off to one side of the event was 320 km s^{-1}. The uncertainty in this value and of the extrapolated starting time of the transient must be stressed since the three points were separated by no more than $R_\odot/10$ at $R/R_\odot \approx 3.50$. However, the velocity agrees with that of the Hα ejection with a starting time at approximately 01 : 41 UT when there were definite Hα structural changes.

The λ5303 observations showed no post-flare loops, and the active region loops seen earlier in the day had disappeared to be replaced by 01 : 26 UT with a tongue-like bright feature matching the Hα structure at that time (Figure 1). The bandpass of the filter was centered on the Fe XIV line throughout so that it is not possible to determine the relative contributions of line and continuum for this emission. At Kitt Peak National Observatory, Harvey and Duvall (1983) visually observed strong white light emission at the flare site. The recorded data (01 : 21 : 41, 01 : 23 : 10, and 01 : 29 : 08 UT) show that the white light feature is of similar size and shape to that observed at Hα and λ5303 wavelengths, at least during the immediate post-flare period.

3.6. Hα AND X-RAY LIGHT CURVES

There were no spatial observations at X-ray energies during this event, but we can compare the Hα brightness variations with results from the HXRBS on SMM. Figure 5 shows the X-ray light curve during the impulsive phase of the flare; the data in separate channels have been integrated over the full energy range (28–485 keV) of the instrument and were taken with 0.256 s time resolution. The data from the low energy channel (25–55 keV) for the full duration of the event (see Figure 6) show both the impulsive and gradual phases of the flare development. In the high energy channels (e.g. 260–480 keV) emission is detected during the impulsive phase only. The Hα maximum intensity in the three main areas of enhanced brightness (see Figure 3) have been plotted in Figure 5 from 01 : 16 : 55 to 01 : 19 : 55 UT. The box at 01 : 18 : 43 UT indicates values which are probably significantly underestimated due to poor image quality at that time.

The curves show that while the intensity in area *B* increased and decreased, the variations in *A* were greater and well correlated with the X-ray spikes. The 12 s time resolution limits the associations to the major peaks, but the enhancement at *C* which could be discriminated above the background on only three frames may have contributed to the minor central X-ray feature. The first major X-ray peak was broader than the second and had two components, but any such structure in the Hα curve is obscured by the uncertainties of 01 : 18 : 43 UT. The duration of the impulsive phase and the interval between the major peaks agree between the two sets of data, the important difference being with the lag time for the Hα curve. The delay cannot be determined to better than 12 s – the Hα sampling rate – but, since the exposure time is almost

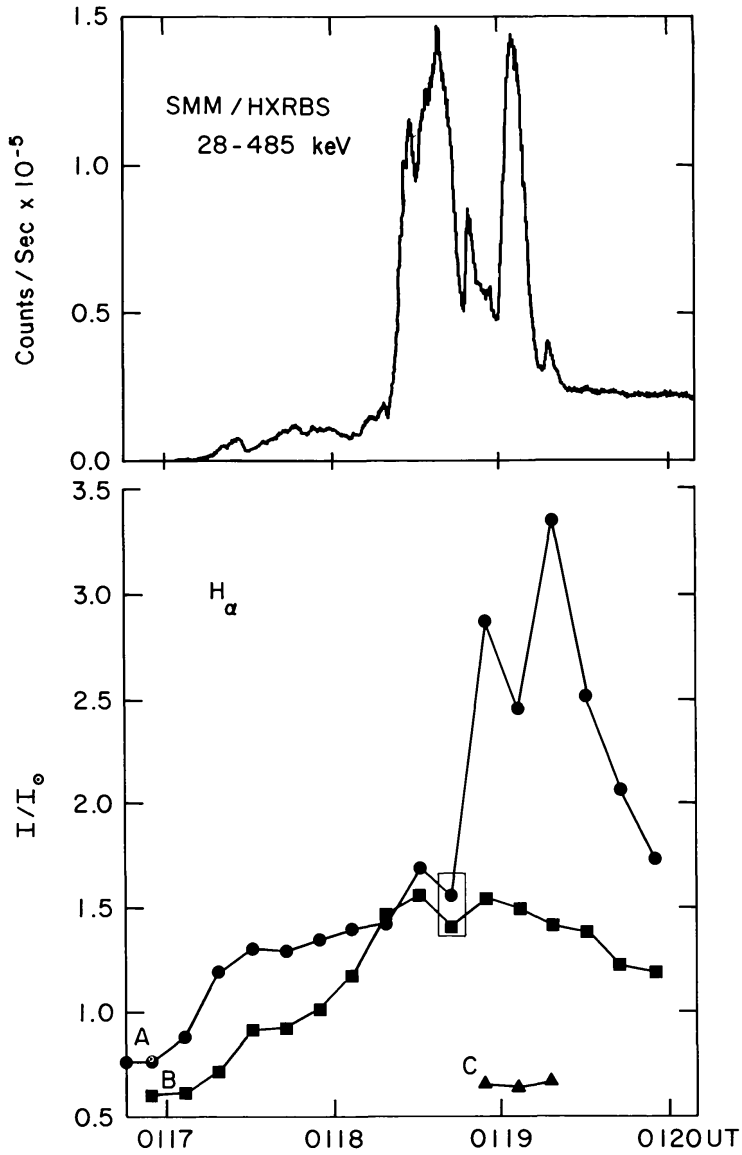

Fig. 5. *Top*: Hard X-ray light curve integrated over the full energy range (28–485 keV) of the HXRBS instrument during the flare impulsive phase. *Bottom*: Hα light curves for maximum intensity in three separate features of the flare event.

instantaneous (0.024 s) and the second X-ray peak and decay are anticorrelated with Hα intensity, it can be considered a real effect.

In Figure 6, we compare the lower energy X-rays emitted throughout the flare lifetime with the integrated Hα intensities within each of three contour levels; these are all plotted on a log-scale. The top section reproduces the HXRBS data from the low energy channel (28–55 keV), while the *B*, *C*, and *D* curves represent the sum of Hα intensities of all points on each exposure where $I/I_0 \geq 0.75$, 1.25, and 2.00 respectively. The 01 : 18 : 43 UT point has been omitted from these plots due to the poor image quality, but it had a value of 205 for curve *B* indicating the probability of a bright kernel at that time. Curve *B*, $\Sigma\,(I/I_0 \geq 0.75)$, includes contributions from the bright kernels, extended chromospheric emission and the loops. The rise time and maximum are in agreement

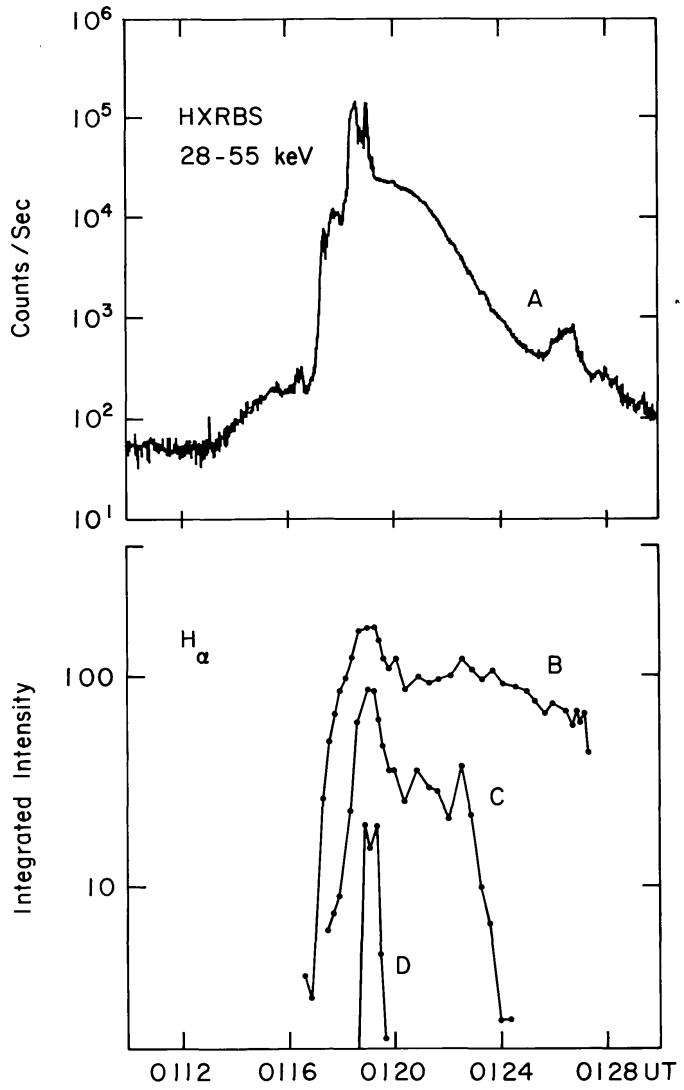

Fig. 6. *A*: X-ray light curve in the low energy band (28–55 keV) of the HXRBS instrument during the flare. *B*, *C*, *D*: Hα light curves of integrated intensity above levels where $I/I_0 \geq 0.75$, 1.25, 2.00, respectively.

with X-ray changes, but the loops that filled after the flare decay caused the Hα intensity to remain relatively high while the X-ray emission in this energy range decayed more rapidly. The late X-ray increase at 01 : 26 UT, which showed also in the 55–126 keV and 126–260 keV channels, corresponds with a marginal Hα increase due to the small feature that brightened near the sunspot as described above (Section 3.4). The fine structure during the impulsive phase and the time delay with respect to the X-ray peaks are associated with the bright kernels – i.e., loop footpoints – where $I/I_0 \geq 2.0$ or 60% maximum intensity. At the times of peak intensity the width of the kernels at the 60% level was 5 arc sec, while the intense cores ($I/I_0 \geq 2.5$) were confined to two and three pixels. Assuming a simple geometry, the flare loops would be around 12000 km high with footpoints of diameter <4000 km.

4. Discussion

The Hα observations of the June 21, 1980, energetic flare have been analyzed in some detail because they provide the only spatially resolved data for this important event and might reveal a clue to the conditions that allow a particular flare to be the site for the release of very high energy. To address this question, we first compare results with those of a limb flare of April 30, 1980, which was well observed by several SMM instruments and has been well analyzed and discussed in the literature (see, e.g., Orwig *et al.*, 1981; Rust *et al.*, 1981; De Jager *et al.*, 1983). The two events were comparable with regard to their location, morphology, and active region structure but the hard X-ray emission differed by orders of magnitude; HXRBS data (≥ 26 keV) showed peak rates of 141 391 c/s and 680 c/s for the June and April flares, respectively (Dennis *et al.*, 1983).

Both flares occurred in decaying active regions, each with a dominant leading sunspot; they were compact events at the west limb with Hα emission at loop footpoints seen against the visible disk. In neither case was there any sign of a filament near the flare position or evidence of preflare filament activity above the limb. The impulsive hard X-rays were associated with the kernels or loop footpoints, while lower energy X-ray emission related to the later, larger loops which filled up and showed evidence of material breaking away at the tops. Each of the Hα flares commenced – after some preflare brightening – with a small mound which extended above the limb and developed a bright knot near the top after a few minutes. The mound in April (June) rose at ≈ 40 (≈ 50) km s^{-1}, accelerated to about 100 km s^{-1} in both cases, reaching heights of 17 000 (8 000) km, respectively; sudden upward acceleration occurred at the times of the hard X-ray bursts.

Although both flares occurred in decaying active regions, each with a dominant leading sunspot, three days before the April flare a group of new spots of opposite polarity grew near the main sunspot and a series of small flares appeared with the new magnetic fields (Rust *et al.*, 1981); new spots and/or flares were not detected prior to the June 21 flare. The coronal response to the two flares was also different. There were strong radio bursts of type III, II, and IV and a coronal transient – as discussed above – with the June event. But on April 30 there were no associated metric radio bursts; NRL Solwind coronagraph data from 22 : 45–23 : 24 UT did not show any effects of a coronal mass ejection above the flare site, although a narrow active streamer was seen at a higher latitude (Howard, 1984). Thus, two obvious differences between the events consist of the greater apparent confinement of the active loops in June and the absence of coronal disturbances following the April flare. A possible reason for the different effects could be the condition of the ambient magnetic field where new flux emerges in the two active regions.

For regions near the west limb, the best estimate of the magnetic field distribution depend on photospheric observations on the disk some days earlier. But the appearance of new sunspots in late April (Rust *et al.*, 1981) was an indication of field adjustments, and these opposite polarity fields are visible on the magnetograms of April 27 (*Solar Geophysical Data*, 1980); on the contrary, there were no such changes in the June region

while it was decaying during the three days before limb passage. It could be expected that there would be a complex of existing magnetic loops above the active region in April, while in June the dominant spot with its strong magnetic field was more isolated; the flare footpoints in June were close to the large sunspot and possibly rooted in the penumbra. This situation agrees with the results of Neidig (1978), who showed how flare emission associated with energetic particles depends strongly on the location of the flare in the active region, suggesting that the strength of the magnetic field governs the energetics. In a study of two ribbon flares, Dwivedi *et al.* (1984) found that the peaks in the hard X-ray bursts were closely related to sunspot proximity and that the power of the energy released into fast electrons depended on how close the corresponding Hα brightening was to the sunspot umbra. This situation was true for the June 21 flare where the intense Hα footpoints closest to the sunspot were associated with the X-ray peaks (cf. area *A* in Figures 3–4). In contrast, the April 30 flare had a much weaker X-ray burst and there is evidence that the Hα brightenings were associated with weaker fields.

The small and intense loops seen with the June flare are also compatible with Vorpahl's (1972) observations that for X-ray-associated flares seen at the limb there was a tendency for Hα confinement prior to the intense kernel brightenings and that impulsive X-ray bursts were more probable when the optical flare exhibited little expansion of material or light.

Another interesting feature is the time delay between X-ray peaks and intensity changes of the brightest Hα kernels during the June 1980 flare impulsive stage; the lower energy X-rays rise and fall together with the integrated brightness of the flare and loops. Time delays between X-ray and optical peaks have been discussed by Vorpahl (1972) and Zirin (1978), who reached different conclusions. Our results agree with Vorpahl's data which were based on light curves traced from off-band Hα exposures; these show only the bright flare kernels which correspond to the hard X-ray sources. For disk flares in the Hα line center, the bright kernel can be obscured by extended chromospheric emission and the overlying loops. The problem is that there should be no delay if the Hα brightenings are the result of excitation by accelerated electrons in the small loops, but if they are excited, for example, by conduction from heated plasma (say 10^8 K) at the top of the loops there could be 10 s required for energy transport down the loop (Brown *et al.*, 1979). Kampfer and Magun (1983) observed differend delays between Hα kernels of a flare and the corresponding microwave bursts and concluded that *different* mechanisms of energy transport might operate in a single flare event. While an Hα delay with the June flare is definite for the second X-ray peak, there is a timing uncertainty regarding the first one, due to the image quality at 01 : 18 : 43 UT. It should be noted that although the maximum brightness was low, the integrated intensity ($I/I_0 \geq 0.75$) reached a peak. Recognizing the uncertainties, we suggest that two energy transport mechanisms may have operated during the flare within the pair of loops that produced the bright Hα footpoints associated with the hard X-ray source.

In summary, we propose the following scenario for the June 21 flare, with times (min) relative to the first X-ray peak (t_0 = 01 : 18 : 30):

(1) (t_0 – 8.5): Magnetic flux tubes emerged within or close to the sunspot umbral field.

(2) (t_0 – 0.8): The loop closest to the sunspot expanded to ≈8000 km, remained confined and became very intense in Hα. The interaction of the emerging field with the ambient field caused energy release and electron acceleration at the top of the loop.

(3) (t_0): Hard X-rays were generated at the footpoint of this loop, energy was transferred in some way to the next loop and a footpoint was excited by a conduction front from the hot plasma in the loop. The Hα brightening occurred later than the corresponding X-ray burst.

(4) (t_0 + 0.8): These loops and others filled by 'evaporation' from the heated chromosphere and emitted lower energy X-rays during the slower decay phase.

(5) (t_0 + 1.0): Evidence of a flare-generated shock wave is shown by the type II radio burst and subsequent coronal transient associated with the ejection of some Hα material at speeds of ≈600 km s^{-1} into the corona. Although the magnetic field appeared to contain most of the Hα ejecta in the low corona, some open field lines were present for the high speed electrons associated with the type III bursts.

(6) (t_0 + 30): Following the flare the Hα material fell back to the surface in a way that indicated a closed field line structure with the appearance of an arcade of loops stretching along the neutral line.

Acknowledgements

The author would like to acknowledge the encouragement of E. L. Chupp to complete this work and the stimulation provided by the Workshop on Impulsive Gamma Ray Flares held at the University of New Hampshire in May 1982. She wishes to thank L. E. Orwig for the HXRBS data presented at that meeting, J. W. Harvey, C. Sawyer, R. T. Stewart, and R. A. Howard for providing supporting data and F. Q. Orrall for many useful discussions regarding this event. Support under NASA grants NGL 12–001–011 and NSG 5326 is acknowledged.

References

Brown, J. C., Melrose, D. B., and Spicer, D. S.: 1979, *Astrophys. J.* **228**, 592.

Chupp, E. L., Forrest, D. J., Ryan, J. M., Heslin, J., Reppin, C., Pinkau, K., Kanbach, G., Rieger, E., and Share, G. H.: 1982, *Astrophys. J. Letters* **263**, L95.

De Jager, C., Machado, M. E., Schadee, A., Strong, K. T., Švestka, Z., Woodgate, B. E., and Van Tend, W.: 1983, *Solar Phys.* **84**, 205.

Dennis, B. R., Frost, K. L., Orwig, L. E., Kiplinger, A., Dennis, H. E., Gibson, B. R., Kennard, G. S., and Tolbert, A. K.: 1983, NASA Technical Memorandum 84998.

Dwivedi, B. N., Hudson, H. S., Kane, S. R., and Švestka, Z.: 1984, *Solar Phys.* **90**, 331.

Harvey, J. W. and Duvall, T.: 1983, private communication.

Howard, R. A.: 1984, private communication.

Kampfer, N. and Magun, A.: 1983, *Astrophys. J.* **274**, 910.

Kane, S. R., Crannell, C. J., Datlowe, D., Feldman, U., Gabriel, A. H., Hudson, H. S., Kundu, M. R., Matzler, C., Neidig, D., Petrosian, V., and Sheeley, N. R., Jr.: 1980, in P. A. Sturrock (ed.), *Solar Flares*, Proceedings of the Second Skylab Workshop, Colorado Associated University Press, p. 187.

Nakajima, H., Kosugi, T., Kai, K., and Enome, S.: 1983, *Nature* **305**, 292.

Neidig, D. F., Jr.: 1978, *Solar Phys.* **57**, 385.

Orwig, L. E., Frost, K. J., and Dennis, B. R.: 1981, *Astrophys. J. Letters* **224**, L163.

Robinson, R. D., Tuxford, J. M., Sheridan, K. V., and Stewart, R. T.: 1983, *Proc. Astron. Soc. Australia* **5**, 84.
Rust, D. M., Benz, A., Hurford, G. J., Nelson, G., Pick, M., and Ruzdjak, V.: 1981, *Astrophys. J. Letters* **244**, L179.
Sawyer, C.: 1982, private communication.
Solar Geophysical Data: 1980, No. 430, Part I, U.S. Department of Commerce, Boulder, Colorado.
Solar Geophysical Data: 1982, No. 459, Part II, U.S. Department of Commerce, Boulder, Colorado.
Vorpahl, J.: 1972, *Solar Phys.* **26**, 397.
Zirin, H.: 1978, *Solar Phys.* **58**, 95.